Tikrit Journal of Engineering Sciences (2024); 31(4): 12-24
DOI: http://doi.org/10.25130/tjes.31.4.2

IRAQI Academic Scientific Journals

ISSN: 1813-162X (Print); 2312-7589 (Online)
Tikrit Journal of Engineering Sciences
available online at: http://www.tj-es.com

TJES Tikrit Journal of Engineering Sciences

Torsional Resistance of High Strength Concrete Filled Steel Tube Beams Stiffened Internally with Steel Bars

Sufyan E. Mutlag *, **Assim M. Lateef**
Department of Civil Engineering, College of Engineering, Tikrit University, Tikrit, Iraq.

Keywords:
Pure torsion; Internal strengthening; High strength concrete; Cross-Rod (CR); Steel tube.

Highlights:

- *Impact of different interior extended surface area of digesters on AD performance.*
- *CD was used as a substrate in digesters under mesophilic conditions.*
- *Digester D has a favored performance due to high extended surface area.*

ARTICLE INFO
Article history:

Received	09 June	2023
Received in revised form	02 Sep.	2023
Accepted	08 Jan.	2024
Final Proofreading	27 May	2024
Available online	24 Nov.	2024

Citation: Mutlag SE, Lateef AM. **Torsional Resistance of High Strength Concrete Filled Steel Tube Beams Stiffened Internally with Steel Bars**. *Tikrit Journal of Engineering Sciences* 2024; **31**(4): 12-24.
http://doi.org/10.25130/tjes.31.4.2

***Corresponding author:**

Sufyan E. Mutlag
Department of Civil Engineering, College of Engineering, Tikrit University, Tikrit, Iraq.

Abstract: The torsional behavior of twelve concrete-filled steel tube (CFST) specimens was experimentally investigated. CFST specimens were reinforced by internal cross-rods with different spacing (0, 50, 100, 150, 200, and 250) mm, different thicknesses of the steel tube (1.5 and 2) mm, and a compressive strength of 65 MPa (high strength concrete). Each sample was tested, and the results were examined. According to the results, the infill concrete prevented buckling failure in CFST specimens. The steel tube and concrete worked together since cutting steel tubes caused diagonal cracks in the infill concrete of CFST specimens. The results also showed that the CFST's torsional moment capacity increased due to the concrete infill, further aiding the steel tubes' performance. Internal stiffening in the steel tubes and concrete infill improved the failure mode, mechanical properties, and CFST specimens' behavior under torsion.

مقاومة عزم الالتواء للأنابيب الفولاذية المملوءة بالخرسانة عالية المقاومة المقواه داخليا بقضبان التسليح

سفيان اسماعيل مطلك، عاصم محمد لطيف
قسم الهندسة المدنية/ كلية الهندسة / جامعة تكريت /تكريت – العراق.

الخلاصة
السلوك الالتوائي لـ ١٢ عينة من الأنابيب الفولاذية المملوءة بالخرسانة (CFST) والمقواة بقضبان متقاطعة داخلية بمسافات متفاوتة (٠، ٥٠، ١٠٠، ١٥٠، ٢٠٠، ٢٥٠) ملم، وسمك متفاوت للأنبوب الفولاذي (١,٥، ٢) ملم ذات مقاومة انضغاط للخرسانة ٦٥ ميجا باسكال (الخرسانة عالية القوة) تم دراستها تجريبيا. تم إخضاع كل عينة للاختبار الكامل، وتم فحص النتائج. ووفقا للنتائج، فإن وجود الخرسانة المملوءة يمنع فشل الانبعاج في عينات(CFST) . أن الأنابيب الفولاذية والخرسانة تعملان معًا لأن قطع الأنابيب الفولاذية يؤدي إلى حدوث شقوق قطرية في الخرسانة المملوءة لعينات(CFST) . تظهر هذه النتائج أيضًا أن قدرة عزم الالتواء لـ CFST قد زادت بسبب المليء بالخرسانة، مما يساعد بشكل أكبر على أداء الأنابيب الفولاذية. أدى استخدام التقوية الداخلية في الأنابيب الفولاذية المملوءة بالخرسانة إلى تحسين وضع الفشل والخواص الميكانيكية وسلوك عينات CFST تحت الالتواء.

الكلمات الدالة: التواء نقي، تعزيز داخلي، خرسانة عالية المقاومة، قضيب متقاطع (CR)، أنبوب فولاذي.

1.INTRODUCTION

1.1.High Strength Concrete

High-strength concrete, defined as having a compressive strength of 41 MPa or above according to ACI 363R-92 [1], is often designed with the qualities of cement and sand and the water-to-cement ratio in mind. High-strength concrete can only be achieved using as little water cementitious material ratio as possible, which always affects the mixture's workability and necessitates the well-compacted concrete mixture using vibration during implementation. Ordinary vibration techniques can be used to compress the concrete mixture to achieve the desired compressive strength of up to 60 MPa at an age of 28 days, provided the components fit together properly. Concrete mix design aims to produce concrete that meets the minimum specified strength, needed process, and durability requirements as cheaply (in terms of engineering value) as possible. When designing high-strength concrete, it may be difficult to determine how much of each ingredient, i.e., cement, sand, and aggregate, to use, as well as how much of each chemical and mineral additive is required. The newest generation of high-range water mixers makes it possible to make concrete of exceptional strength. High-strength concrete's greater load-bearing capability and the ability to lower column diameters and beams have made high-rise buildings (often above 30 stories) possible. In addition to lowering the loads associated with foundation design, a building with low dead loads benefits the end user monetarily because columns take up more rentable space and less wasted space.

1.2.Concrete Filled Steel Tube

Concrete-filled steel tubular (CFST) buildings have many advantages over other types of construction due to their robustness, ductility, and ability to absorb force. Additionally, concrete-restrained steel tubes with high steel tube rigidity prevent concrete from being crushed (steel tube benefit) [2-5]. Shuttering is not required for concrete construction, reducing time and money spent. Because of these benefits, concrete-filled tubular structures are commonly used in civil engineering projects. Concrete-filled steel tubular constructions have been extensively used and studied in China. Recent years have witnessed a proliferation of books released into the public domain [6-11]. Local requirements and rules of practice were also produced to aid in the design process. Focusing on recent advancements in China, the present paper surveys the current state of the art for concrete-filled steel tube constructions. The current methods of design in various countries are briefly discussed. The present work studied the development of concrete structures and searched for projects using concrete-filled steel tube (CFST) techniques.

1.3.Component Behavior

Figure 1 displays three typical column cross-sections: a circular hollow section (CHS), a square hollow section (SHS), and a rectangular hollow section (RHS). The dimensions of the steel tube, denoted as D, B, and t, respectively, indicate the outer, inner, and wall dimensions. Square and rectangular cross-sections are more prone to local buckling than circular ones, offering the most effective concrete core confinement. The extensive use of concrete-filled steel tubes with SHS and RHS in construction is driven by their aesthetic value, strong cross-sectional bending stiffness, and the convenience they provide in beam-to-column connection design. It is well known that concrete has a substantially higher compressive strength than tensile strength. Compressive strength is improved further when subjected to bi-axial or tri-axial stress. While structural steel has a lot of strength when stretched, its shape can be changed when compressed. Steel and concrete are used in concrete-filled steel tube members, which make the most of both materials' inherent strengths. With the steel tube providing confinement and the concrete core providing support, local buckling of the steel tube is reduced.

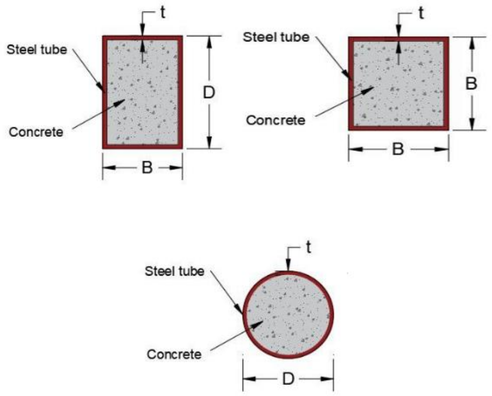

Fig. 1 Typical Concrete-Filled Steel Tubular Cross Sections.

1.4.Materials for Concrete-Filled Steel Tubes

1.4.1.Steel

Steels, such as high-performance, fire-resistant, weathering, ordinary carbon, high-strength, and "mild" steel, are among the many options for the steel used to make concrete-filled tubular members. National standards [12] outline common sections in China, including their dimensions and dimensional restrictions. In terms of mechanical properties, structural steel can be found in standards, such as GB/T 700 [13] for carbon steel and GB/T 1591 [14] for high-strength low-alloy steel. A set of rules for the design of structural steel in China, GB 50017 [15]. The concert wall thickness should be higher than the specified thickness to last the steel tube structure. According to the DBJ/T 13-51 standard, steel tubes must have an outside diameter of 100 mm or more [16]. It is recommended that the concrete-filled steel section have a larger diameter-to-wall thickness ratio than the hollow section due to the enhanced local buckling capability caused by the concrete. Chinese design standard GB 50010 [17] specifies that if the diameter-to-wall thickness ratio (D/t) is outside the allowed range, extra stiffeners must be made and supplied.

1.4.2.Concrete

The filled concrete in CFST buildings can be either regular or high-strength concrete. Since the enclosed tube will not allow surplus water to escape, the concrete’s ratio, i.e., water to cement, must be carefully managed. High-strength concrete cannot have a water-to-cement ratio higher than 0.3. Ductility and energy dissipation were very high in experimental concrete-filled steel tubular beams using HSC, and the load-carrying capacities were comparable to those of beams with standard concrete [9, 18]. Better structural performance can be achieved by appropriately matching the steel and concrete strengths [7, 17]. Steel with higher strength should be used with similarly strong concrete, and steel with lower strength should be used with similarly weak concrete. For instance, a concrete compressive strength of 55-65 N/mm² would be suitable if the steel tube's yield strength falls between 235 and 345 N/mm². When the steel tube's yield strength exceeds 345 N/mm², the concrete's compressive strength should be at least 60 N/mm² [18].

1.5.Static Performance

When a steel tube filled with concrete is subjected to torsion, the inner concrete undergoes compression, while the steel tube experiences tensile force along the diagonal. The core concrete prevents the steel tube from buckling, and the resulting "truss action" creates more open space. As shown in Fig. 2, when torsion is applied, the hollow steel tube clearly demonstrates shear buckling [19]. Experiments on long CFST members under sophisticated load procedures by Perea et al. [20] were conducted regarding the narrow CFST sections. According to the findings, the CFST columns conducted were more effective, according to the American specification. Bridges and large-span buildings are just two examples of the composite concrete-filled steel tube members applications. Han et al. [21] studied the effects of several tube shapes, beginning curvature, tubular lattice members made of concrete and filled with steel have their nominal slenderness ratios, cross-sectional patterns, and brace patterns calculated. Experimental results demonstrated that filling chord tubes with concrete greatly improved the load-bearing capacity, initial stiffness, and curved latticed elements’ ductility. The specimen of the hollow tube had 30%-40% less axial compressive strength than its concrete-filled counterpart [21]. The experimental results also revealed an increase in the ratio of initial curvature to nominal slenderness. The curved concrete lattice specimen's ultimate strength and stiffness were diminished. Throughout its useful life, concrete will experience creep and shrinkage, affecting the CFST members [7, 22, 23]. Steel tube columns filled with concrete under prolonged loads have had their time-dependent behavior studied, and a theoretical model to account for shrinkage and creep effects has been proposed [23]. The core concrete's shrinkage and hydration heat become noticeable when the concrete-filled steel tube's cross-sectional profile increases. Concrete-filled steel tubes were subjected to experimental analysis of their hydration heat and shrinkage [24, 25].

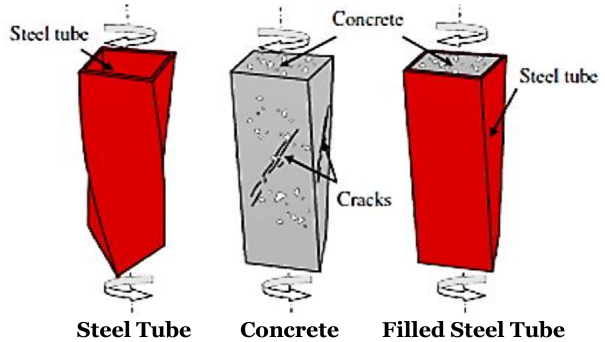

Fig. 2 Schematic Failure Modes of Steel Tube, Concrete, and CFST under Torsion.

2.AIM OF THE STUDY

Combining multiple ways to strengthen the beams from the inside is unusual because torsion strengthening of reinforced concrete-filled steel tube beams is typically done externally. The primary objectives of this study are conducting an experimental analysis of the effect of interior cross-rod steel reinforcement on (CFST), and estimating the potential increase in torsion strength as a function of tube thickness and the number of cross-rods (CR).

3.EXPERIMENTAL PROGRAM

3.1.Specimen's Details

An experimental program was conducted in the Civil Engineering Lab at Tikrit University. Twelve Tests were conducted on cast specimens of beams. For this research, one served as a reference beam and was denoted by (NST1-C1 and NST2-C2) for two thicknesses, and four beam specimens used variable spacing between internal cross-rebar (CR) to increase their strength. These beams were denoted by (HSTx-y), i.e., (x) is the thickness of the tube, and (y) is the spacing. Each specimen's breadth, depth, and length (in millimeters) were 100×100×2000, and they were cast out of regular concrete. Each beam specimen's cross rod was reinforced with (8 mm) bars, with the number of cross-rods inside the beam as one of the crucial adopted factors, i.e., 50mm, 100mm, 150mm, 200mm, and 250mm. The first beam specimen was a reference beam (R-B) without an internal cross-rebar. The names, measurements, and other details about the tested beams are listed in Table 1, Table 2, and Figs. 3 - 5.

3.2.Supply Items

3.2.1.Cement

Tables 3 and 4 display the physical and chemical parameters of Ordinary Portland Cement (Type1), which complies with Iraqi regulations (I.O.S.No.5.1984).

3.2.2.Fine Aggregate

Like all concrete combinations, this study employed natural sand. In accordance with Iraqi specification (I.O.S. No.45, 1984), the fine aggregate sieve analysis results are displayed in Table 5.

3.2.3.Coarse Aggregate

For the present research, crushed gravel that could not be larger than 12.5 mm was used. Iraqi specification (I.O.S. No. 45, 1984) limits and coarse aggregate grading, as shown in Table 6.

3.2.4.Water

Clean tap water was used in the present study.

3.2.5.Steel Reinforcement

The steel diameter calculation method is outlined in ASTM A 615 [14]. Table 7 shows the mechanical properties of the steel bars.

3.3.Concrete Mixing

As shown in Fig. 3 (a), all specimens' concrete was made by mixing the necessary ingredients in a revolving mix. Several trial mixtures yielded the required strengths, and new varieties of concrete were developed to attain the required cubic strengths of 65 MPa at 28 days (high-strength concrete). Fig. 3 (b) displays the slumping test result prior to casting (150 mm). The molds were fully lubricated and placed vertically on a flat, stable ground. The casting process was conducted as shown in Fig. 3 (c) for reference beams and Fig.3 (d) for strengthened beams. Table 8 displays the specifications of the mixture.

Table 1 Details of Specimen's Beams (Group A).

Designation of Beam	Dimensions (mm) d	w	L	t	Spacing between Internal Cross-Rebars	Description
HSCT1-C1					0	Reference beam
HSCT1-25					250 mm	Strengthening beam @250mm
HSCT1-20	100	100	2000	1.5	200 mm	Strengthening beam @200mm
HSCT1-15					150 mm	Strengthening beam @150mm
HSCT1-10					100 mm	Strengthening beam @100mm
HSCT1-5					50 mm	Strengthening beam @50mm

Table 2 Details of Specimen's Beams (Group B).

Designation of Beam	Dimensions (mm) d	w	L	t	Spacing between Internal Cross-Rebars	Description
HSCT1-C1					0	Reference beam
HSCT1-25					250 mm	Strengthening beam @250mm
HSCT1-20	100	100	2000	2	200 mm	Strengthening beam @200mm
HSCT1-15					150 mm	Strengthening beam @150mm
HSCT1-10					100 mm	Strengthening beam @100mm
HSCT1-5					50 mm	Strengthening beam @50mm

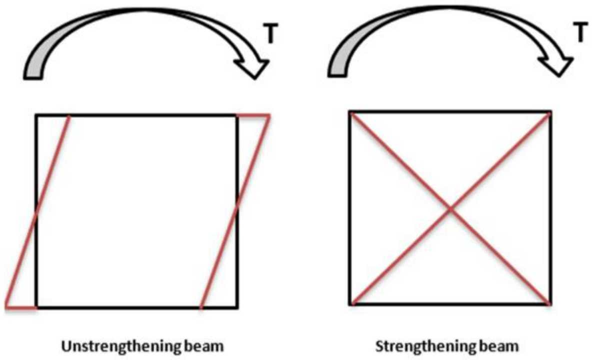

Fig. 3 Torsion Effects on the Unstrengthen and Cross-Rod-Strengthened Beams.

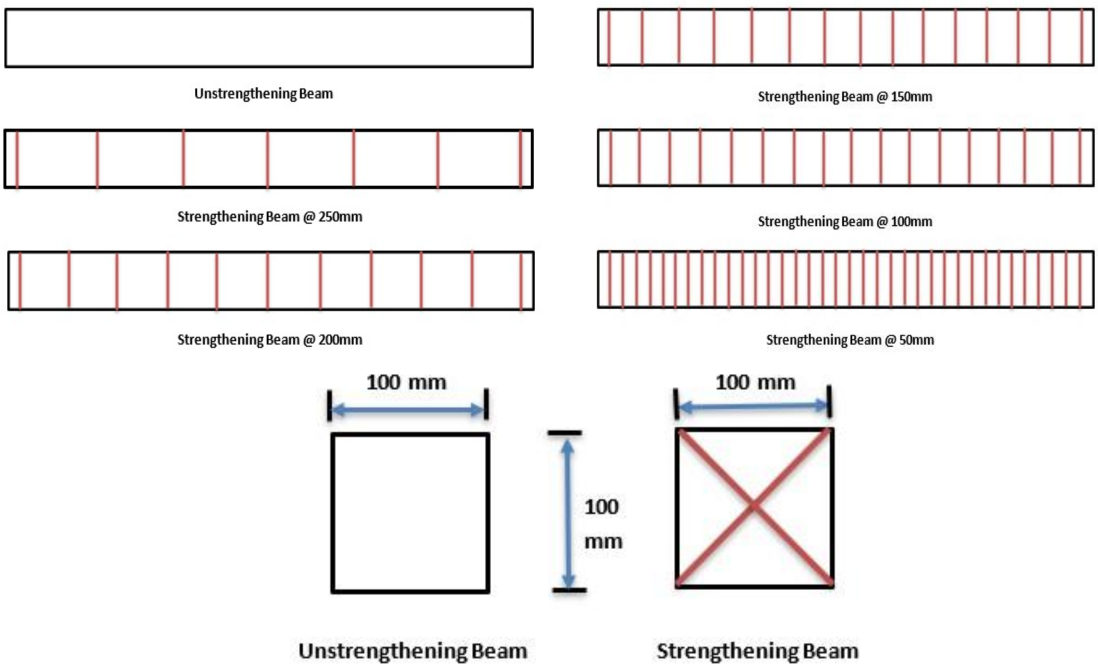

Fig. 4 Reference Beam and Specifications for the Internal Cross-Rebar Steel Reinforcing.

Table 3 The Chemical Properties of Cement*.

Oxides composition	Content %	Limit of Iraqi specification No. 5/1984
(CaO)	60.36	-
(AlO3)	20.17	-
(SiO2)	4.66	-
(Fe2O3)	3.63	-
(MgO)	4.12	(5%MAX)
(SO3)	2.39	(2.5%MAX)
(Loss on Ignition), (L, O, I)	2.87	(4%MAX)
(Insoluble material)	1.32	(1.5MAX)
(Lime Saturation Factor), (L, S, F)	0.85	(0.66-1.02)

* The Civil Engineering Labs in Tikrit University conducted testing.

Table 4 The Physical Properties of Cement*.

Physical Properties	Test Results	Limit of Iraqi specification No. 5/1984
(Specific surface area), (Blaine method) (m^2/kg)	308	(230 m^2/kg) lower limit
(Setting time), (vacate apparatus)		
(Initial setting) (hrs.: min)	2:15	(Not less than 45 min)
(Final setting) (hrs.: min)	4:10	(Not more than 10 hr.)
(Compressive strength), (MPa)		
(For 3day)	(28.8)	(Not less than 15 MPa)
(For 7 day)	(34.2)	(Not less than 32 MPa)

* The Civil Engineering Labs in Tikrit University conducted testing.

Table 5 Analysis of Fine Aggregate Using a Sieve *.

No.	Sieve size	Cumulative Passing %	Limit of IQS NO. 45/1984 for zone No. 3
1	4.75-mm (No.4)	90.90	90-100
2	2.36-mm (No.8)	88.89	85-100
3	1.18-mm (No.16)	78.75	75-100
4	600-µm (No.30)	67.74	60-79
5	300-µm (No.50)	16.83	12-40
6	150-µm (No.100)	4.37	(Limit of IQS NO. 45/1984 for zone No. 3)
		Fineness modulus =2.44	

* The Civil Engineering Labs in Tikrit University conducted testing.

Table 6 Analysis of Coarse Aggregate Using a Sieve *.

No.	Sieve Size	Coarse Aggregate %	Iraqi specification No. 45/1984
1-	14mm	100	90-100
2-	10mm	75.6	50-85
3-	5mm	3.4	0-10
4-	pan	0	-

* The Civil Engineering Labs in Tikrit University conducted testing.

Table 7 The Characteristics of Rebar Made of Steel.

Diameters of bars(mm)	Yield stress(f_y) (MPa)	Ultimate stress (f_u) (MPa)
8mm	580	670

Table 8 The Requirements for the Mixture.

Constituent	Water	Cement	Fine Sand	Coarse Aggregate	SPR
Amount (kg/m3)	173	540	587	1069	0.5%

Table 9 Hardened Properties of High-Strength Concrete.

Mixture	Compressive Strength (MPa)		Splitting strength (MPa)	Flexural Strength (MPa)
	7 Days	28 Days	28 Days	28 Days
High strength concrete	39.55	65.36	7.74	9.88

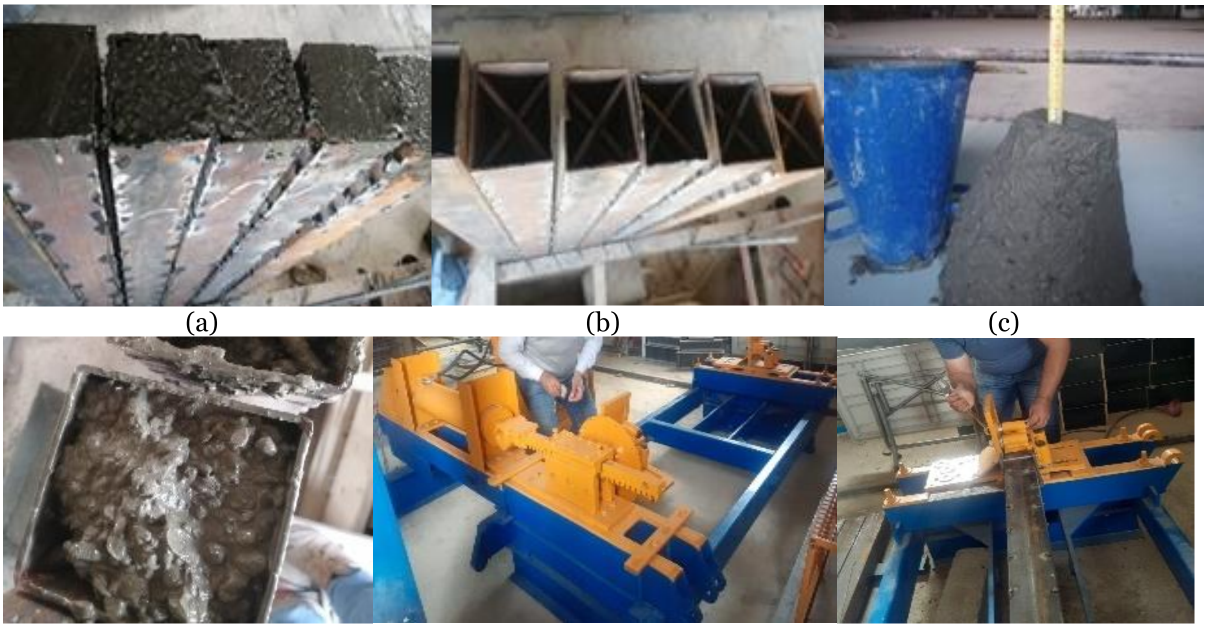

(a) (b) (c) (d) (e) (f)

Fig. 5 Strengthening Beams with Welding and Concrete Mix and a Cast of Beams, then Slump Test.

3.4.Test Setup and Instrumentation

Figures (6) – (9) depict the test setup in detail. The beam testing machine was built to apply a torsion moment to test specimens. Steel frames were securely fastened to the ends of beam examples to create the torsional arm. The distance from the axis of the steel shaft to the end edge was 250 millimeters. Using a hydraulic jack and an electric motor capable of producing a maximum load of 250 kN, all specimens were tested for their maximal twist moment (torque) and crack resistance. Due to its design, i.e., held at two points by the bearings, the beam could freely rotate even when torque was applied. To release the sample from its restraint, the fixed support was inserted, and the support was moved beneath the bearing. A hydraulic jack generated the torque by putting a standard load along a steel shaft (dish serrated) connected to the torsional arm. It is important to remember that the gadget was created entirely by the authors.

Fig. 6 Beam Test.

(a) (b)

Fig. 7 General View.

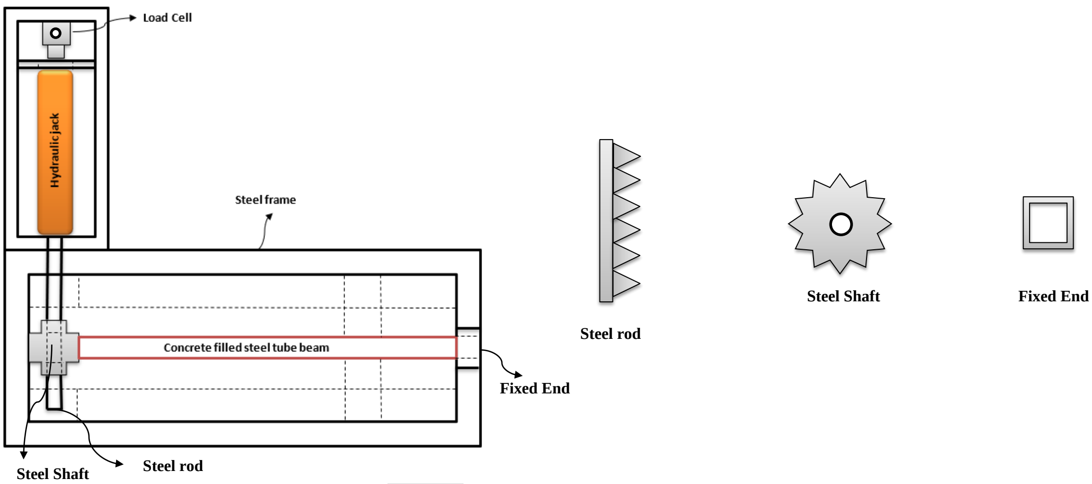

Fig. 8 Outline (Top View).

HST1-C1

HST1-5

HST1-10

HST1-15

HST1-20

HST1-25

Fig. 9 (a) Specimen After Testing.

HST2-C2

HST2-5

HST2-10

HST2-15

HST2-20

HST2-25

Fig. 9 (b) Specimen After Testing.

3.5.Twist Angle Measurements

Gradually applying the load allows for determining the maximum twisting angle and torsional capabilities. Data was recorded using a user-supplied data logger connected to an LVDT sensor and load cells to send information about loads and lateral displacements. Taking readings in the up and down directions allowed the sensors to calculate the beam's twist angle. By measuring the distances between the center of the beam and the LVDT sensor, the angular deviations can be determined by dividing the measured displacement by the LVDT readings, i.e., equivalent to 150 mm, and solving for the resulting twisted angle yields:

Trigonometrically, the twist angle equals $\tan^{-1}$ (LVDT sensor reading divided by 150). The distance between the cross-center sections and the LVDT location was 150 mm. Figure 10 shows the twist angle (Θ) measurement.

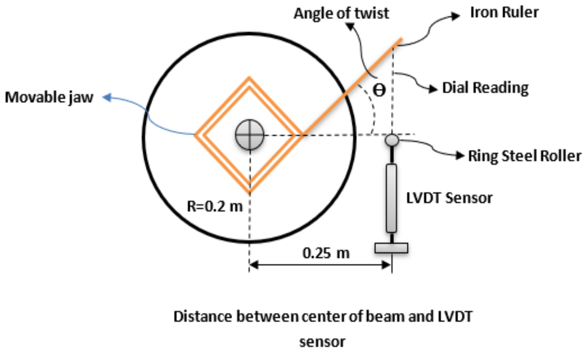

Fig. 10 Measurements of the Twisting Angle.

Fig. 11 Steel Tubular Specimens Filled-Concrete Test.

4.DISCUSSION AND FINDINGS

4.1.The Ultimate and Cracking Loads

Torsion tests had been performed on beam samples under a constant load. The length of the beam support at both ends was always the first place a crack appeared in any of the test specimens. Table 10 and Fig. 11 detail the data for the cracked (Pcr), ultimate loads (Pu), crack tension (Tcr), and ultimate tension (Tu). When comparing the cracked torque value (Tcr) of the tested beams (HST1-25), (HST1-20), (HST1-15), (HST1-10), and (HST1-5) to that of the reference beam (HST1-C1), it is found that the strengthened internal cross-rods increased the value by 2.997%, 4.09%, 5.72%, 29.59%, and 33.46%, respectively. Table 11 and Fig. 11 detail the results for the cracked (Pcr), ultimate (Pu) loads, crack tension (Tcr), and ultimate torsion (Tu). For a set of tested beams (HST2-25), (HST2-20), (HST2-15), (HST2-15), and (HST2-5), the cracked torque value (Tcr) was higher by 10.15%, 14.1%, 25.8%, 35.12%, and 50.82%, respectively, than the reference beam (HST2-C2). This result suggests that the inner cross-rod strengthening can withstand bigger strains and, thus, provide more torsion resistance. For tested beam specimens (HST1-25), (HST1-20), (HST1-15), (HST1-10), and (HST1-5) the ultimate torsion (Tu) was increased by 9.88%, 15.9%, 26.18%, 35.34%, and 51.28%, respectively, compared to the control beam (HST1-C1), and internally strengthened by 25, 20, 15,10, and 5 internal cross-rods. The ultimate torsion (Tu) of the test beams (HST2-25), (HST2-20), (HST2-15), (HST2-10), and (HST2-5) was increased by (6.46%), (17.43%), (21.13%), and (27.97%), respectively, compared to the control beam (HST2-C2). As a result, the inner cross-rebar strengthening could withstand more stress and improve torsion strength. According to the data, there was no separation of the cross-rod from the concrete, and the tested beams exhibited the maximum torsional strength at 5 spacing (CR). Internal cross-rebars allowed for transmitting greater lateral forces inside the planes of torsional stresses, increasing the beam sections' efficiency and resilience against torsional stresses [26].

$$T = P \times arm \quad (kN.m) \qquad \textbf{(1)}$$

Figure 2 shows that the cross bars are crucial in resisting torsion. When subjected to torsion, the reference beam without reinforcement exhibits slips in the corners of the beam, whereas the beam with reinforcement exhibits no such creep because it contains cross bars. The beam's resistance to torsion is enhanced by the fact that one of them acts as a strut and tie.

4.2.Torque-Angle of Twist Behavior

Figures 12 and 13 show the maximum torque relative to the twisting angle for a regulated and strengthened beam. Beam deformation capacity can be drastically modified using internal cross-rod strengthening. From the onset of the first cracks to the point of failure, the test data showed a steady increase in the twist angle of about 0.31 degrees. The strengthened beams had a smaller twist angle than the control beams at the same stress just before the first crack appeared. While some outliers were at the end of the torque-twist curves for strengthened beams, overall, their behavior was consistent with control beams. Cross-rods (CRs) prevent cracking by resisting the torque applied to the beams, resulting in uniformly sloping curves after the cracking phase. Compared to the control beam (HST1-C1), the ultimate twist angle of the strengthened specimens increased by 13.42, 15.44, 19.46, 23.49%, and 25.55 degrees, as shown in Tables 12 and 13, respectively, and a comparison to the control beam (HST2-C2) resulted in (25.52%), (35.41%), (19.79%), (16.667%), and (25%), respectively. A possible explanation for this behavior is that adding a transverse steel cross-rod inside the beam, which allowed for a greater amount of torque to be transferred, however, raised the beam's corresponding angle of twist.

Table 10 The Ultimate Torque Relates to the Cracking of Every Evaluation Beam Specimen (group A).

Beam	Thickness t mm	Pcr (kN)	Pu (kN)	Arm (m)	Tcr (kN.m)	Tcr N-Ren Beam measures an increase (%)	Tu (kN.m)	Tu N-Ren Beam measures an increase (%)
HST2-C2	2	67.76	118.85	0.25	16.94	-	29.712	-
HST2-25	2	74.64	126.52		18.66	10.15	31.63	6.46
HST2-20	2	77.32	131.88		19.33	14.1	32.97	10.97
HST2-15	2	85.24	139.56		21.31	25.8	34.89	17.43
HST2-10	2	91.56	143.95		22.89	35.12	35.99	21.13
HST2-5	2	102.2	151.88		25.55	50.82	37.97	27.79

Table 12 The Ultimate Torque Relates to the Cracking of Every Evaluation Beam Specimen (group A).

Beam	(Tu) (kN.m)	(θu) (rad/m)	(%) Increase of (θu)
HST1-C1*	22.27	0.149	-
HST1-25	24.47	0.169	13.42
HST1-20	25.81	0.172	15.44
HST1-15	28.1	0.178	19.46
HST1-10	30.14	0.184	23.49
HST1-5	33.69	0.187	25.5

*Reference Beam

Table 13 The Ultimate Torque Relates to the Cracking of Every Evaluation Beam Specimen (group B).

Beam	(Tu) (kN.m)	(θu) (rad/m)	(%) Increase of (θu)
HST2-C2*	29.712	0.192	-
HST2-25	31.63	0.241	25.52
HST2-20	32.97	0.26	35.41
HST2-15	34.89	0.23	19.79
HST2-10	35.99	0.224	16.667
HST2-5	37.97	0.24	25

*Reference Beam

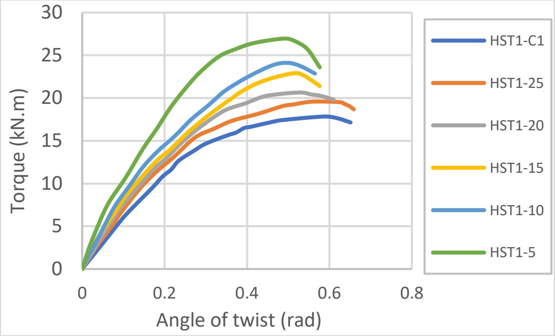

Fig. 12 The Tested Beams' Torque-to-Rotation-Angle Relationship (group A).

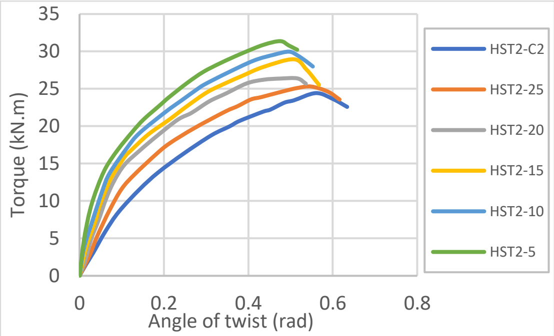

Fig. 13 The Tested Beams' Torque-to-Rotation-Angle Relationship (group B).

4.3.Mechanisms of Failure

Torsional moments were the cause of failure for all tested beams; in all cases, the crack began within the initial one-third of the available time and grew progressively longer. As the moment of torque grew, the cracks that began on the beam's vertical sides made their way inward along its axis. The principal cracks were angled at 30°–45° from the beam's longitudinal axes [27]. After the cracking had occurred, the load was increased. In addition, its tension-carrying capacity vanished when it was close to its failure stage. The quantity of cracks they generate and the manner in which they penetrate the beams were also variable. Figure 7 (a) and (b) depicts the failure mechanisms of the control beam (HTX-Y) and the strengthened beam (HSTX-Y) when subjected to pure torsion, increasing the amount of strengthening in the loaded beams, so too had the number of cracks. Increased tension led to more cracks in the strengthening beams than in the control beam (HTX-Y). Furthermore, it was found that the beam with the 5 cm internal stiffeners had an equal distribution of cracks as the number of internal cross-rods (ICR) increased.

5.CONCLUSIONS

In summary, the study focused on the effect of internal reinforcement of cross-rebars of steel tubular beams concrete filled, including the torsional behavior, cracking load, ultimate load, cracking torque, ultimate torque, towing angle, and beams' failure modes. The following can be deduced from the experimental results of the tested beams:

1- Strengthening the section's torsion capacity using internal cross-rod steel reinforcement appears simple and effective.

2- More steel cross-rod reinforcements inside the structure boosted its final torsion capacity.

3- Increasing the number of internal cross-rebars being increased (ICR) further enhanced beam characteristics when the angle of torsion (Ø) before failure was higher.

4- When the top of a square SRCFST specimen was subjected to torsion, the failure was localized near the top. The failure mode of all specimens evaluated was invariant throughout a wide range of stress conditions and steel reinforcement cross-section types. In contrast to the types of steel reinforcement used in the cross-section, the loading directions slightly affected cracks in the concrete's core.

5- The variation in the T-curve of specimens under different loading routes was essentially the same. A little variation in torsional rigidity appeared between cross-section varieties of steel reinforced using the same steel reinforcement ratio.

REFERENCES

[1] Russell HG, Anderson AR, Banning JO, Cantor IG, Carrasquillo RL, Cook JE, Frantz GC, Hester WT, Saucier KL, Aitcin PC. **State-of-the-Art Report on high-Strength Concrete**. *ACI Committee* 1997; **363**: 92, (1-55).

[2] Ali HA, Salman WD. **Behavior of Hybrid CRRP-Concrete-Steel Double Skin Tubular Column under Axial Load**. *Diyala Journal of Engineering Sciences* 2020; **13**(1): 106–117.

[3] Hussien TA, Salman WD. **Experimental Investigation on RC Columns Confined by Jacket with Geopolymer Adhesive**. *Diyala Journal of Engineering Sciences* 2022; **15**(2): 103–113.

[4] Naser AF. **Evaluating The Connection Areas Between Bricks Walls and Concrete Columns in Confined Masonry Buildings in Iraq**. *Diyala Journal of Engineering Sciences* 2017; **10**(2): 12–26.

[5] Salman WD, Salman SM. **Fibrous Geopolymer Adhesive Jackets for Confining of Reinforced Concrete Columns**. *Diyala Journal of Engineering Sciences* 2021; **14**(3): 119–130.

[6] Cai SH. **Modern Steel Tube Confined Concrete Structures**. *Beijing: China Communications Press* 2003; **12**(3): 121-136.

[7] Han LH. **Concrete Filled Steel Tubular Structures-Theory and Practice**. *Journal of Fuzhou University* 2016; **2001**(6): 34.

[8] Han LH, Yang YF. **Modern Technology of Concrete-Filled Steel Tubular Structures.** 2nd ed., Beijing: China Architecture & Building Press; 2007.

[9] Han LH, Tao Z, Wang WD. **Advanced Composite and Mixed Structures—Testing, Theory and Design Approach**. Beijing, China: Science Press 2009.

[10] Tao Z, Yu Q. **New Types of Composite Columns—Experiments, Theory and Methodology**. Beijing: Science Press; 2006.

[11] Zhong ST. **The Unified Theory of Concrete-Filled Steel Tubular Structures: Research and Application**. Tsinghua University Press 2006.

[12] 50205-2001 GB. **Code for Acceptance of Construction Quality of Steel Structures**. 2001.

[13] 700-2006 G. **Carbon Structural Steels**. 2006.

[14] GB/T 1591–2008. **High Strength Low Alloy Structural Steels**. Standard Press of China 2008.

[15] GB 50017–2003. **Code for Design of Steel Structures**. Beijing. *Standard Press of China* 2003.

[16] DBJ/T13-51-2010. **Technical Specifications for Concrete-Filled Steel Tubular Structures (Revised Version)**. *Fuzhou, China: The Housing and Urban–Rural Development Department of Fujian Province* 2010.

[17] Standard C. **GB50010-2010 Code for Design of Concrete Structures**. 2010.

[18] Han L-H, Yao G-H, Zhao X-L. **Tests and Calculations for Hollow Structural Steel (HSS) Stub Columns Filled with Self-Consolidating Concrete (SCC)**. *Journal of Constructional Steel Research* 2005; **61**(9): 1241–1269.

[19] Han LH, Yao GH, Tao Z. **Performance of Concrete-Filled Thin-Walled Steel Tubes under Pure Torsion**. *Thin-Walled Structures* 2007; **45**(1): 24–36.

[20] Perea T, Leon RT, Hajjar JF, Denavit MD. **Full-Scale Tests of Slender Concrete-Filled Tubes: Axial Behavior**. *Journal of Structural Engineering* 2013; **139**(7): 1249–1262.

[21] Han LH, He SH, Zheng LQ, Tao Z. **Curved Concrete Filled Steel Tubular (CCFST) Built-Up Members under Axial Compression: Experiments**. *Journal of Constructional Steel Research* 2012; **74**: 63–75.

[22] Uy B. **Static Long-Term Effects in Short Concrete-Filled Steel Box Columns under Sustained Loading**. *Structural Journal* 2001; **98**(1): 96–104.

[23] Han LH, Tao Z, Liu W. **Effects of Sustained Load on Concrete-Filled Hollow Structural Steel Columns**. *Journal of Structural Engineering* 2004; **130**(9): 1392–1404.

[24] Han LH, Yang YF, Li YJ, Feng B. **Hydration Heat and Shrinkage of HSS Columns Filled with Self-Consolidating Concrete**. *Fourth International Conference on Advances in Steel Structures* 2005; Shanghai, China: p. 647–652.

[25] Ibraheem OF, Mukhlif OA. **Behavior of Reinforced Concrete Plates under Pure Torsion**. *Tikrit Journal of Engineering Sciences* 2021; **28**(1): 84–97.

[26] Abdullah AI, Lateef AM. **Novel Torsional Reinforcement of Concrete Beams Utilizing Cross-Rod Steel Reinforcement**. *Tikrit Journal of Engineering Sciences* 2023; **30**(3): 49–58.

[27] Abdulrahman MB, Jomaa'h MM, Alsubari B, Abdulaali HS, Alqawzai S. **Torsional Behavior of RC Beams with Transverse Openings Strengthened by Near Surface Mounted-Steel Wire Rope Subjected to Repeated Loading: Torsional Behavior**. *Tikrit Journal of Engineering Sciences* 2022; **29**(4): 79–89.